Int J Earth Sciences (Geol Rundsch) (2001) 90:753–768
DOI 10.1007/s005310000172

ORIGINAL PAPER

Jan H. Behrmann · Achim Kopf

Balance of tectonically accreted and subducted sediment at the Chile Triple Junction

Received: 8 December 1999 / Accepted: 16 October 2000 / Published online: 9 March 2001

Abstract An active oceanic spreading ridge is being subducted beneath the South American continent at the Chile Triple Junction. Mass balance estimations to characterize temporal and spatial variations in the frontal accretion, or underplating and subduction of sediments since the Late Miocene, were made using seismic and drill-hole data. At 200 km north of the triple junction, almost 80% of the sediment on the downgoing Nazca plate are subducted. Sediment subduction rate decreases towards the triple junction because of a low in sedimentation rates as the flank of the spreading ridge approaches the trench. At the triple junction, the forearc is almost completely destroyed by spreading ridge collision and subduction erosion. Less than 12% of the available sedimentary input is accreted. South of the triple junction, where the spreading ridge passed 6 Ma ago, a large fraction (>60%) of the sediment on the incoming Antarctic plate has been scraped off and was frontally accreted to the Chile forearc. Spreading ridge subduction leaves a distinctive geological fingerprint, and has a large impact on the mass balance of the subduction zone. However, the high rates of change in the process may make this fingerprint hard to detect in fossil convergent orogens. In the ridge collision zone the sediment supplied to the trench, and the amount of sediment subducted, show strong and distinctive variations on a 1- to 5-million-year time scale. On a 10-million-year time scale, sediment subduction to the Earth's mantle is reduced by spreading ridge collision, caused by the need of the overriding forearc to regain a low angle of taper by frontal accretion.

J.H. Behrmann (✉)
Geologisches Institut, Albert-Ludwig-Universität Freiburg, Albertstrasse 23B, 79104 Freiburg, Germany
E-mail: behrmann@uni-freiburg.de

A. Kopf
Géosciences Azur, B.P. 48, 06235 Villefranche-sur-Mer Cédex, France

Keywords Accretion · Chile · Forearc · Plate tectonics · Subduction

Introduction

Convergent margins are among the most active tectonic environments on Earth. Unravelling the geological and tectonic history of the deforming system provides insights into the plate boundary geometry and dynamics, and imposes constraints on long-term mass transfer at convergent plate boundaries. At present, forearc and accretionary prism structure is best constrained by seismic profiles and deep sea drill cores. Age information from the drill-cores also provides key evidence for the dynamics of sedimentation on the downgoing plate, and for accretionary wedge growth. On the basis of a plate kinematic reconstruction for the SE Pacific–South America area, estimates of sedimentation rates, reflection seismic data and drill core information, this study aims to estimate sediment subduction and sediment accretion along the southern Chile margin, where an actively spreading mid-oceanic ridge is currently undergoing rapid subduction beneath a continental plate (Fig. 1). This is the only modern example of a process that must have often occurred in past orogenies, and is of paramount importance in understanding crustal growth, mountain building, and recycling of crustal material into the Earth's mantle.

Spreading-ridge subduction leaves distinctive stratigraphic and structural signatures in the geological record of the overriding plate, including (1) rapid forearc uplift and subsidence (e.g. DeLong and Fox 1977; DeLong et al. 1979), (2) regional metamorphism and elevated thermal gradients (e.g. Sisson et al. 1989), (3) a hiatus in arc magmatism (e.g. Ramos and Kay 1992), (4) anomalous near-trench magmatism (Marshak and Karig 1977), (5) localized forearc extension, subsidence, and subduction erosion (e.g. Herron et al. 1981; Barker 1982; Behrmann et al. 1994; Bourgois et

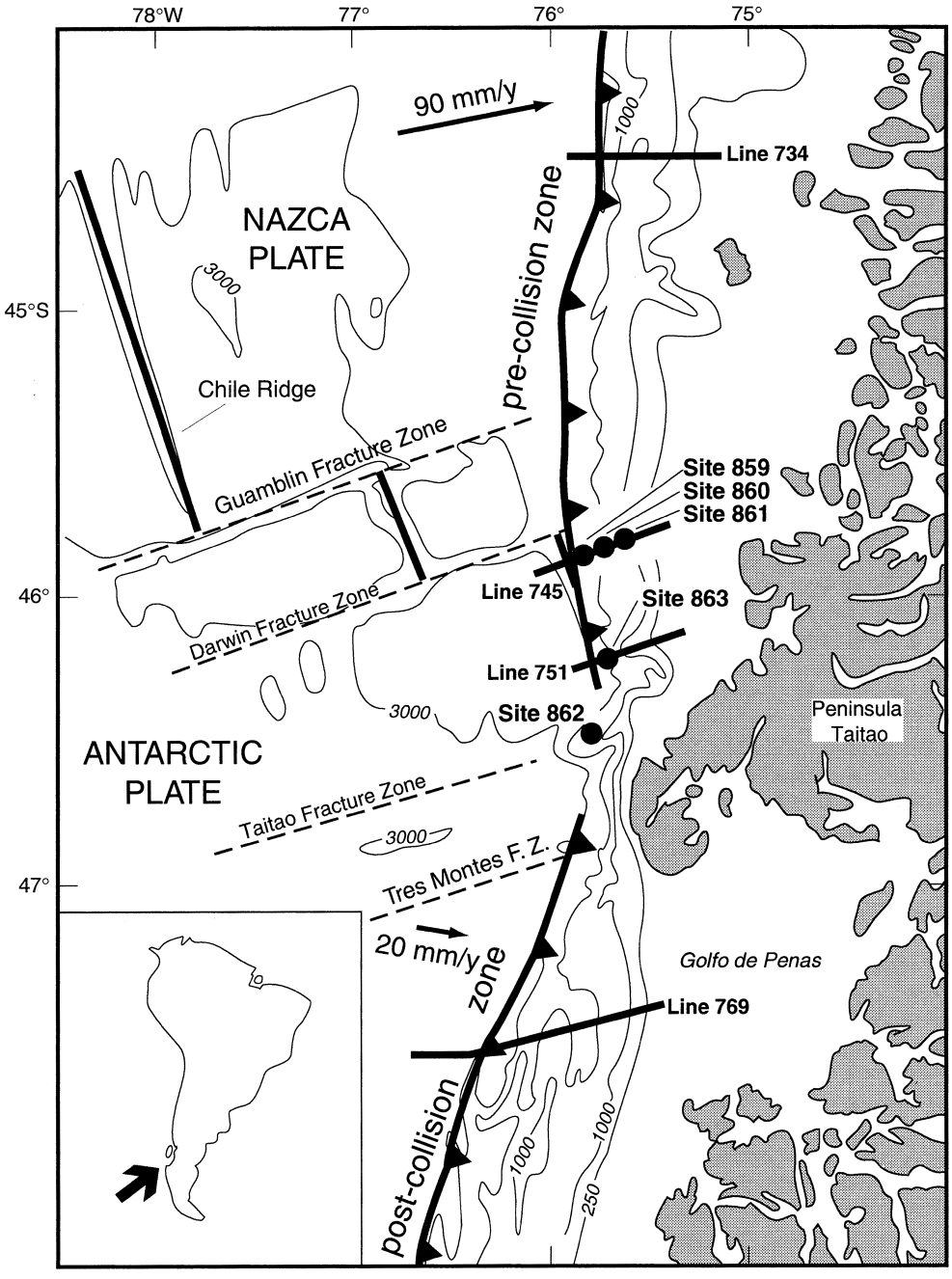

Fig. 1 Tectonic sketch map of the Chile Triple Junction area. *Bold lines* show actively spreading segments of the Chile Ridge. *Dashed lines* mark transform zones. The position of the deformation front along the forearc of southern Chile is marked by the *barbed line*. Reflection seismic lines and ODP Leg 141 drill sites are indicated

al. 1996), (6) hydrothermal fluid flow and possible gold mineralization (Haeussler et al. 1995), and (7) ophiolite obduction (e.g. Casey and Dewey 1984; Forsythe et al. 1986).

Volume balance of subducted and accreted rock masses: reviewing the problem

Volume balancing studies along convergent margins generally aim to estimate the proportions of sediment supplied, accreted and subducted (e.g. Hilde 1983; von Huene and Lallemand 1990; von Huene and Scholl 1991). The hypothesis of sediment subduction was developed to account for material at mantle depths supplying island arc volcanics (Coats 1962) well before the plate tectonics paradigm was formulated and became widely accepted. Approximately a decade later, it was proposed that subduction-related tectonic erosion removed continental crustal rocks (e.g. Miller 1970; Murauchi 1971). Both, sediment accretion and subduction erosion are divided into frontal and basal addition or removal of material (e.g. Scholl et al. 1980; von Huene and Scholl 1991). Besides different processes of frontal accretion of sediment scraped off from the incoming, subducted plate (e.g. Karig and Sharman 1975), large amounts of sediment can pass the deformation front and be added subcrustally. This

process is known as underplating (e.g. Platt et al. 1985). Missing material, margin truncation and subsidence are indications of both frontal and subcrustal subduction erosion. The collision of high-relief structures (seamounts, ridges, etc.) is thought to dismember the forearc and, thereafter, is responsible for the transport of material to mantle depths (e.g. von Huene and Lallemand 1990; Gutscher et al. 1999). Different parameters (e.g. the trench sediment thickness, the dip angle of the downgoing slab, the critical taper of the accretionary wedge, the basal friction caused by the width of the subduction channel, etc.) are thought to control the amount of material undergoing the different processes (e.g. von Huene 1986; Willett 1992; Kukowski et al. 1994; von Huene et al. 1994; Cloos and Shreve 1996).

Major problems in obtaining reliable estimates are (1) the lack of data (of tolerable quality) from deeper crustal levels that cannot be reached by scientific drilling and geophysical surveys, (2) the number of simplifications that have to be made (e.g. steady-state sediment input over time), and (3) the large variety of interacting processes and parameters that take place at convergent margins. In the case of the Chile Triple Junction area, we feel that the array of available seismic reflection profiles and line-drawing interpretations, together with ODP Leg 141 drilling data (Behrmann et al. 1992), and a comparatively simple plate kinematic situation, provides an acceptable basis for a mass balance assuming steady-state conditions since the latest Miocene up to recent time. The virtue of the study reported here is not so much to yield exact figures, but to provide a semi-quantitative view of solid mass fluxes during an important tectonic process that has shaped active plate margins in the geological past.

Geological setting of the Chile Triple Junction

At 46°S latitude, the actively spreading, NW–SE-trending Chile Ridge, dividing the oceanic Nazca and Antarctic plates (e.g. Herron et al. 1981) is presently being subducted beneath the South American margin (Fig. 1). Plate kinematic reconstructions concerning the Nazca, Antarctica and South American Plates suggest a first collision of the Chile Ridge with the Chile trench at ~14 Ma B.P. (e.g. Cande et al. 1982, 1987). Since then, the overall motion of the triple junction has been northward, resulting in the subduction of ridge segments and transform faults (Cande and Leslie 1986). Because of the northward migration of the triple junction the South Chile convergent plate boundary can be divided into a pre-collision zone to the north, a collision zone in the immediate vicinity of the triple junction, and a post-collision zone in the south (Fig. 1).

Numerous tectonic and magmatic phenomena in the overriding South American plate have been attributed to ridge collision. The continuous uplift of the Andes during the past 7 million years (and especially the area around the Chile triple junction) has been related to crustal thickening as a result of plate-scale compressional tectonics (Howell 1989) and magmatism (Pankhurst et al. 1992; Bourgois et al. 1996). Evidence for this from geological processes on land was found from various studies: (1) uplift of upper Tertiary marine basins (Flint et al. 1994) and the underlying arc and forearc basement (Forsythe and Prior 1992), (2) large-scale deformation and size reduction of the forearc by subduction erosion (Behrmann et al. 1994; Bourgois et al. 1996), (3) distinct uplift, cooling and exhumation on land dated by apatite fission track analysis (George and Hegarty 1995), (4) critical depth of intrusion of young plutons (Pankhurst et al. 1992), and (5) the age distribution pattern of flood basalt fields (Ramos and Kay 1992; Lagabrielle et al. 1994).

Viewed on a large scale, Cretaceous igneous and older metamorphic basement rocks are in contact with the young and recent forearc sediments (e.g. Miller 1970; Rutland 1971). Missing material (e.g. Hussong et al. 1976; Scholl et al. 1977) as well as discrepancies in volume balance calculations (e.g. von Huene and Scholl 1991; Bourgois et al. 1996) were identified and interpreted as indicating long-term subduction erosion and transfer of significant amounts of crustal rock volume into the Earth's mantle at the Andean convergent margin. For the Isla Mocha area, ~1,000 km north of the Chile Triple Junction, Bangs and Cande (1997) implied that sediment accretion and non-accretion are episodic, and controlled mainly by the amount of sediment transported from the forearc into the trench and, in the long term, the fraction of sediment accreted may be comparatively low. This conclusion has to be taken into account when focusing our attention on the balance of subducted and accreted sediment in the immediate vicinity (up to 200 km north and south; see Fig. 1) of the Chile Triple Junction.

Input data

The influence of the subducting spreading ridge on the forearc structure is displayed by cross sections interpreted from multi-channel seismic reflection surveys with RV *Conrad* along traverses perpendicular to the continental margin (Fig. 1). These time-migrated sections provided one important basis for this study. Seismic reflection lines imaging the Chile margin before (Lines 734, 745), during (Line 751) and after ridge collision (Line 769) show the highly variable structure and size of the forearc wedges at the different latitudes (Fig. 2). For each of the profiles studied, an interpretation is shown in Fig. 3. Despite the lack of pre-stack migration and depth processing (with only filtering and deconvolution, time migration, but no removal of multiple energy), the data show the main

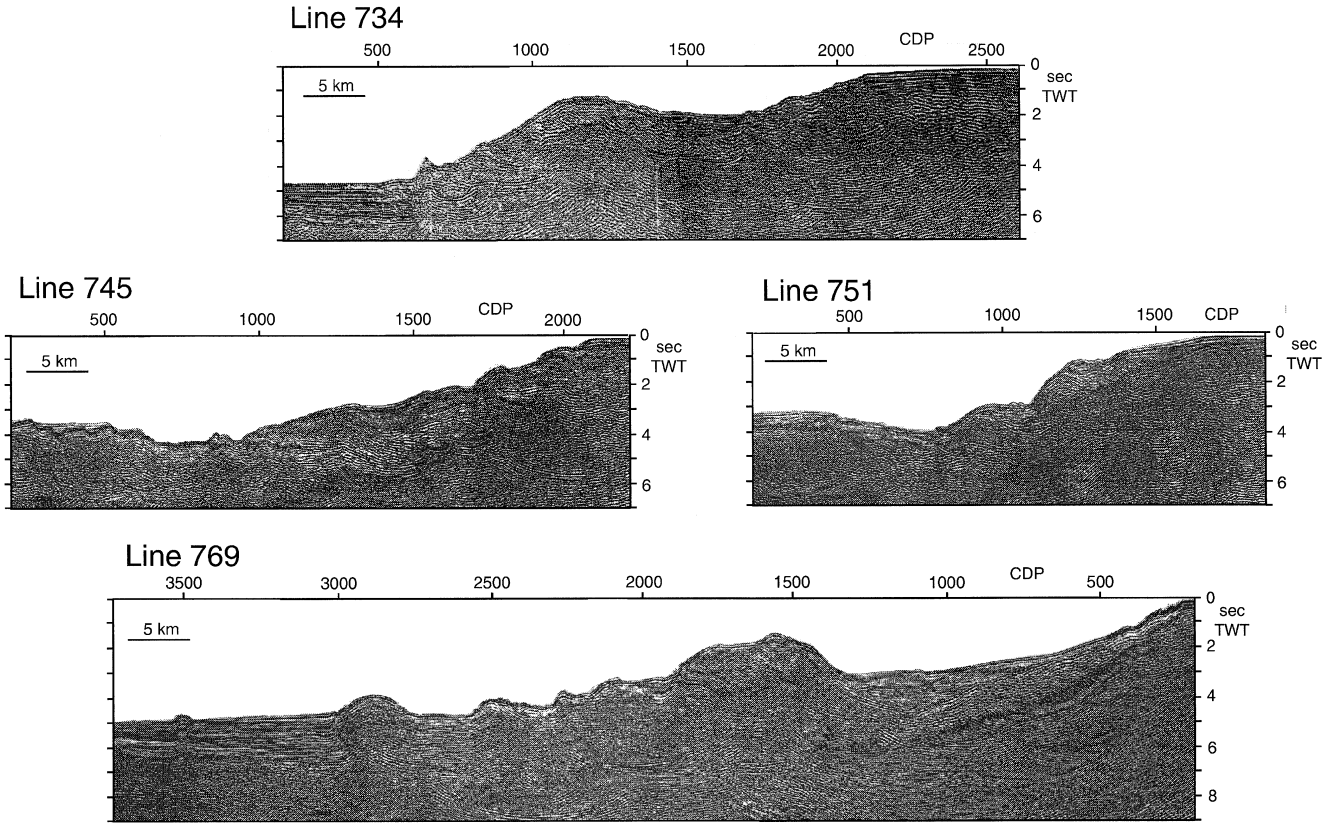

Fig. 2 Migrated seismic lines 734, 745 (pre-collision zone), 751 (collision zone), and 769 (post-collision zone). See Fig. 1 for locations

sedimentary and tectonic units, and the cross sectional areas of the accreted rocks can be determined with reasonable confidence. The sedimentary sequence on top of the oceanic crust (on the left in all sections of Figs. 2 and 3) as well as the slope apron show undisturbed layering, largely seafloor parallel, but sometimes thinned towards the edges of horsts or grabens. The accreted sediments are characterized by an irregular seismic pattern, inferring tectonic shortening, folding and faulting. Imbrication and backthrusting can be seen along some of the profiles, with a body of accreted material overlying the prominent 'basement' reflector. The inferred continental basement rock beneath this reflector exhibits no internal structure. In the section immediately north of the triple junction (Line 745; compare Figs. 1, 2 and 3), some of the incoming sediment can also be traced down beneath the forearc crustal wedge. This feature is more clearly imaged in the pre-stack depth migrated section 745 published by Bangs et al. (1992).

Along Line 734, located ~200 km north of the triple junction, a comparatively large accretionary wedge overrides the incoming, 7 Ma-old Nazca crust at the deformation front, and is backthrust onto the continental forearc basement (Figs. 2, 3a). A thick sedimentary trench sequence on the incoming Nazca plate reflects high long-term mass transfer rates into the Chile trench. Landward-dipping thrust faults are the main structural feature of the accretionary wedge (Fig. 2 and 3a; see also Bangs and Cande 1991). Landward of a prominent outer-arc high, a forearc basin with undeformed sediments of presumed Neogene–Quaternary age overlies the backthrust strata (Figs. 2 and 3a). In the toe area of the prism, the sediment appears to be underthrust; however, this underthrust sequence is difficult to trace to depth without better imaging. With no drill-hole data available there is no direct proof for a young age of the accretionary wedge, as along Line 745 further south (see below). However, the absence of a thick slope sediment cover seaward of the forearc basin, and the observation that active thrusts cut up to the subsea surface, indicate that the accretionary wedge is young and probably being actively built (Fig. 2). A smaller accretionary wedge is developed along Line 745 located south of the Darwin fracture zone (cf. Fig. 1) and ~30 km north of the triple junction (Figs. 2 and 3b). The active spreading ridge is ~5 km seaward of the deformation front, and (assuming constant plate movements) will interact with the forearc in ~100,000 years time (Bangs et al. 1992). The tectonic structure of the wedge allows clear distinction between a backthrust sliver, and an underthrust (or underplated) sliver of accreted strata. Much of the structural interpretation

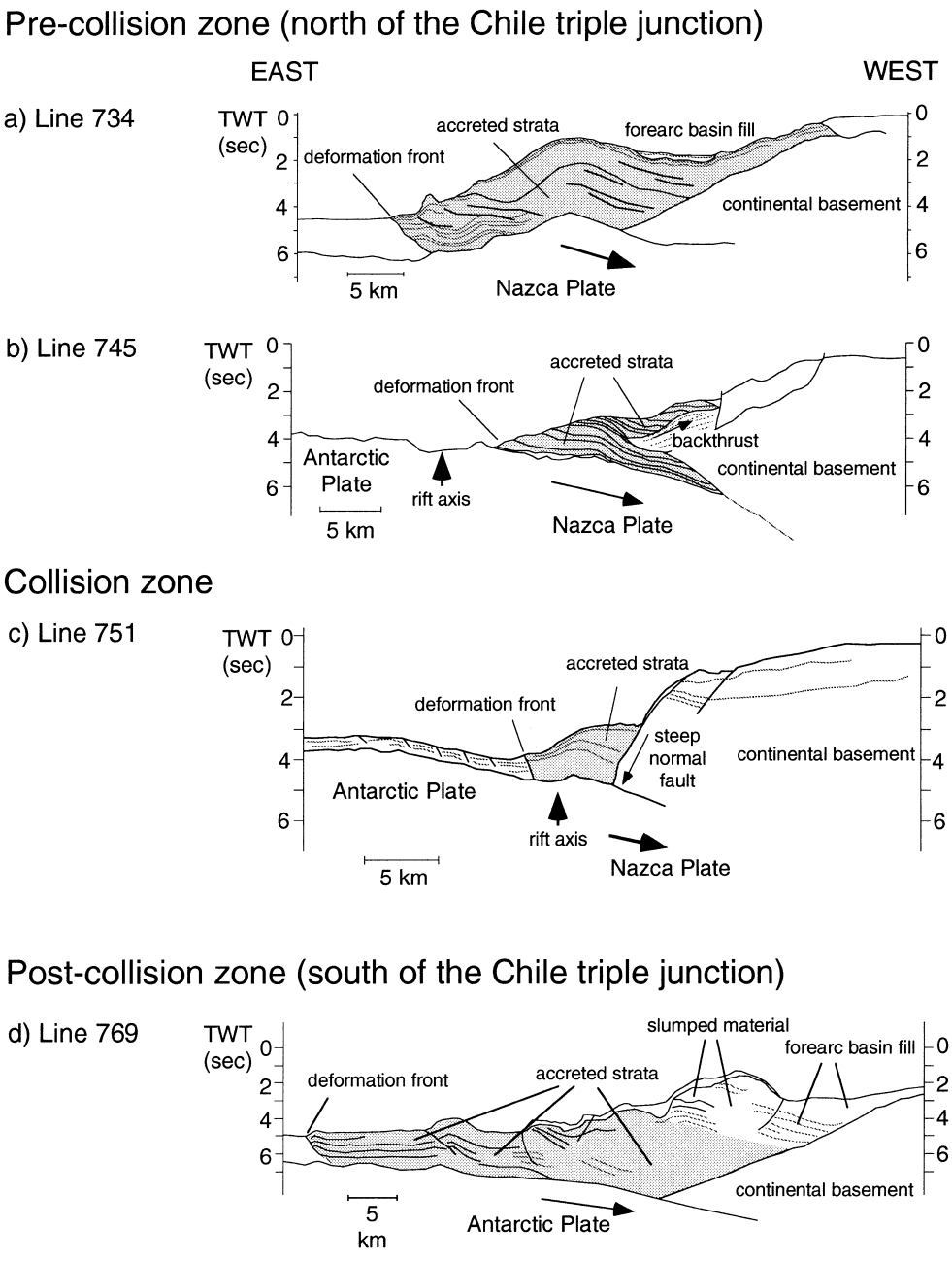

Fig. 3 Interpretations of seismic sections **a** 734, **b** 745, **c** 751, and **d** 769

of Line 745 is corroborated by ODP Leg 141 drill-hole data (Behrmann et al. 1992, 1994).

Yet further south, Line 751, (see Figs. 2 and 3c), images the dramatic change in forearc geometry that accompanies collision of the spreading ridge. A small accretionary prism bounded towards the continent by a steep normal fault is underlain by the subducted rift axis. Seaward of the deformation front the ocean floor is characterized by horst-and-graben structures tilted towards the ridge axis, with vertical displacements of up to 1,000 m. The extensional deformation that accompanied spreading ridge subduction deformed both the slope sediments and the accreted succession, which is characterized by randomly oriented reflectors. The comparison with the wedge-buttress structure further north suggests that the forearc has suffered tectonic erosion along the leading edge of the South American plate (cf. Figs. 2 and 3c). Along the southernmost profile, Line 769 at 47.35°S latitude (Fig. 1), the forearc geometry changes again. An extensive accretionary prism defined by both seaward- and landward-dipping imbricate thrusts is seen (Figs. 2 and 3d). A thick sediment pile is apparently completely accreted at the present time. The top of the 9-Ma-old oceanic crust of the Antarctic plate east of the present deformation front can be identified as a strong reflector dipping at an angle shallower than in the collision zone (see Fig. 3c). According to our interpretation, the eastern-most part of the accretionary wedge was backthrust onto the continental buttress for a few kil-

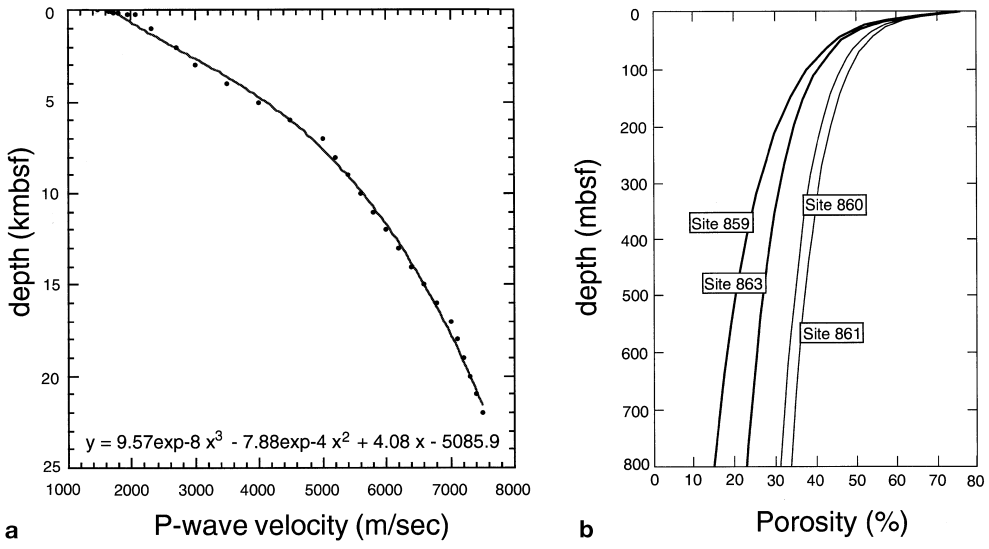

Fig. 4 **a** 'Best fit' velocity-depth (*kmbsf* kilometres below sea floor) function calculated from p-wave velocities obtained from ODP Leg 141 drill-cores (Behrmann et al. 1992) and seismic refraction data acquired during the CONDOR cruise (von Huene et al. 1997). **b** Porosity-depth (*mbsf* meters below sea floor) functions for ODP sites 859–861 and 863 (after Kopf 1995)

ometres, and is overlain by a forearc basin containing a thick succession of layered sediments.

Four of a total of five sites drilled during ODP Leg 141 at the Chile Triple Junction (Behrmann et al. 1992, 1994) were located along Lines 745 and 751 (Fig. 1). The sediments recovered consisted dominantly of silty clay, clayey silt and nanno-fossil ooze of exclusively Plio-Quaternary age. Homogeneity concerning their facies and biostratigraphic dating infer a similar depositional facies for the last 5 Ma (Behrmann et al. 1992). Palaeo-depth reconstructions using benthic foraminifera assemblages reveal a complex history of vertical movements as a result of the subduction of the spreading ridge (Behrmann et al. 1994). Although the toe region along Line 745 (Site 859) shows no evidence for large vertical movements since Pliocene time, both the deeper part of the sedimentary column of the middle (Site 860) and upper slopes (Site 861) have undergone major uplift during the Pliocene (on the order of 2,000 m). Further south near the triple junction, strong subsidence of the upper part of the sedimentary succession of Site 863 is suggested (Behrmann et al. 1994). The sediments below reflect a deposition at water depths similar to the modern trench and therefore suggest a history of frontal accretion, imbrication, folding and uplift, which was followed by a major subsidence event. The geometry of the accretionary wedge at Line 751 appears to be the result of extensional tectonics along the prominent normal fault, and subduction erosion of both sediments and continental crust (Fig. 3c).

Methods and models

This section will be divided into three parts, which follow the logic flow as well as the chronological order the work has been carried out. In the first part, the forearc sections are velocity–depth converted. In the second part, synthetic sediment basin fills on the Nazca and Antarctic plates are constructed from the plate kinematic framework and sediment accumulation rates. Finally, the third part shows the results from balance calculations, which are transformed into solid rock mass using sediment porosity data derived from ODP Leg 141 core samples (Behrmann et al. 1992)

Time–depth conversion of forearc sections

As no electronic files of the seismic data were available, graphic time–depth conversion of the time sections were carried out to enable quantitative estimates. Two types of data were used to define the conversion procedure. First, p-wave velocity data were obtained from each drill core as part of the shipboard routine during Leg 141 (Behrmann et al. 1992). In addition, borehole measurements with a sonic tool obtained p-wave velocity data from Sites 859, 860 and 863. As a result of the shallow terminal depths of ODP drilling the velocity data set was extended using data from wide-angle seismic refraction experiments with RV *Sonne* off northern Chile (the CONDOR cruise; Flueh et al. 1995, 1998). These data provided valuable constraints for the deeper velocity structure. A 'best fit' velocity–depth function was calculated from the combined data sets of the ODP and CONDOR cruises (Fig. 4a), and we feel that, at least for the upper 15 km of continental forearc crust, this function provides a robust approximation. The resulting graph was found to be very similar to two-dimensional velocity models derived from depth focusing analyses during pre-stack depth migration of seismic lines, which were acquired with RV *Conrad* slightly to the north (J. Diaz, personal communication 1998). Time–depth conversion of the seismic lines was carried out by selecting prominent reflectors from the structural interpretations (Fig. 3), and converting two-

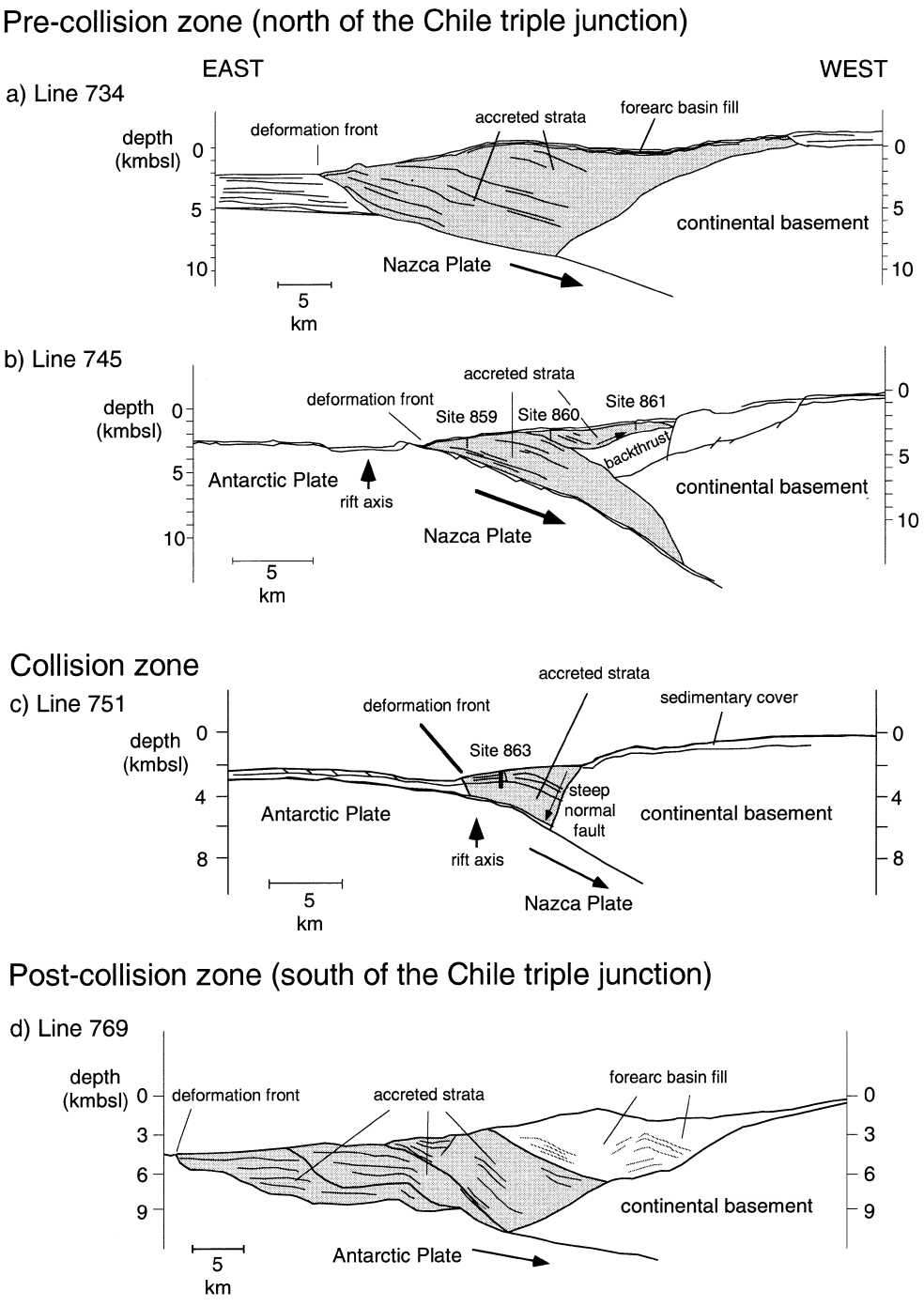

Fig. 5 Depth-converted cross sections of seismic lines **a** 734, **b** 745, **c** 751, and **d** 769. See text for discussion

way travel time (TWT) to depth using the velocity–depth function (Fig. 4a). The depth converted sections and their interpretations are shown in Fig. 5, and are discussed below. Cross sectional areas of the accreted rocks (shaded areas in Fig. 5) are given in Table 1.

Basin models and reconstructed sedimentary input

The total amount of material that was initially deposited into the oceanic basin is the counterpart to the component of sediment added to the continent by off-scraping and accretion. One important variable for the synthetic basin models is their width in the approximate east–west direction. This variable is controlled by the spreading rate of the Chile Ridge and the subduction rates of the Nazca and Antarctica plates at the southern Chile trench. Relative plate motions in this system have varied little in the last 5 million years (see Cande and Leslie, 1986). The plate kinematic vector triangle depicted in Fig. 6a is derived from published data, and essentially follows Cande and Leslie (1986), who summarised and reviewed earlier work (e.g. Klitgord et al. 1973; Chase 1978; Minster and Jor-

Table 1 Uncompacted and compacted cross-sectional areas of the sediments in the accretionary wedge and the synthetic basin along Lines 734, 745, 751, and 769. The *asterisk* marks models based on sedimentation rates from ODP Leg 141 drill-hole data

Tectonic setting		Accretionary wedge			Synthetic basin		
Location	Line	Cross-section area (km^2)	Solid area, max. (km^2)	Solid area, min. (km^2)	Cross-section area (km^2)	Solid area, max. (km^2)	Solid area, min. (km^2)
Pre-collision	734	168.6	126.5	122.2	890.6	611.2	592.0
Pre-collision	745	53.9	47.7	43.3	456.3	368.8	337.2
Pre-collision	745* max.	53.9	47.7	43.3	157.7	124.3	
Pre-collision	745* min.	53.9	47.7	43.3	73.7		53.3
Collision	751	17.5	15.7	13.8	166.3	132.8	121.6
Post-collision	769	288.2	223.2	204.1	517.2	355.6	341.9

dan 1978; Herron et al. 1981; Cande 1983; Forsythe et al. 1986). Although lateral movements are part of the assembly process at ocean margins (e.g. Beck 1983), material transfer parallel to the direction of plate movement was assumed. This assumption appears viable, as the component of trench-parallel motion is small, and is not partitioned into distinct zones of strike-slip shearing in the southern Chile forearc (Behrmann et al. 1994).

The synthetic basin models (Fig. 7) have three horizontal axes. The lower one is a horizontal kilometre scale that serves as a reference for the position of Nazca and/or Antarctica oceanic basement of a given age (upper axis). Age of oceanic crust is derived from the crustal age–space distribution shown in Fig. 6b (see also Murdie et al. 1993). The middle axis indicates the position of the deformation front (the leading edge of the overriding South American plate) in the past relative to its present position. The overthrusting of the South American plate terminates sedimentation at a given instant in time. Together with sedimentation rates (see below) all three parameters control the thickness of sediment that can be accumulated at a given point in the basin.

Average sediment accumulation rates are estimated from the thickness of the sedimentary cover over oceanic crust of a known age (Fig. 6b). For seismic lines 734, 745, 751 and 769, estimates were made from sediment thicknesses on the oceanic crust seaward of the deformation front, using the depth-converted cross sections (Fig. 5). Sedimentation rate estimates are up to 485 m/Ma for a period from latest Miocene (6 Ma B.P.) to present, with the exception of Line 751 right in the ridge collision zone where intense Pleistocene mass wasting into the trench (Behrmann et al. 1994) leads to a rate of 1,400 m/Ma. For two reasons this estimate has to be treated with due caution, however. In a recent reflection seismic survey providing better spatial resolution, Bourgois et al. (2000) demonstrated that this thick sediment cover of the trench area is not developed everywhere. Lines 9 and 10 of Bourgois et al. (2000) show thick sediment cover, whereas Line 7, further to the north, shows thick sediment cover on the Chile Ridge shoulders only, but not in the trench. Also note that the sedimentation rate inferred from Line 751 is only constrained for the Pleistocene; a comparatively short time span. We interpret the high sedimentation rate as representing the immediate consequences of ridge collision and resulting forearc uplift and dissection. Sediment accumulation rate estimates are summarized in Table 2. Near the trench at Line 745, the sedimentary cover is very thin owing to the extremely low age of the incoming oceanic crust (150,000 years), making this sedimentation rate estimate (350 m/Ma) very uncertain. Therefore, the Plio-Quaternary sediment accumulation rates based on biostratigraphic markers in ODP drill cores have been used for comparison (Behrmann et al. 1992). As shown in Table 3, accumulation rates vary from 41–260 m/Ma for the Pleistocene and 47–287 m/Ma for the Pliocene. Thus the 350 m/Ma estimate from the reflection seismic traverse may be too large.

A problem is to realistically estimate the sedimentation rates prevailing during the Miocene, which forms a small but important fraction of the oceanic basin fill along Lines 734 and 745 (Fig. 7). During ODP drilling, no Miocene sediment has been recovered, although the forearc wedge was penetrated completely at one site (Site 862, Fig. 1; see also Behrmann et al. 1992). However, because of the age of the crust beneath the seafloor, a Miocene cover has to be

Table 2 Sediment accumulation rate estimates from reflection seismic data

Sediment accumulation rates from reflection seismic data				
Tectonic setting	Line	Thickness of incoming sediment (m)	Age of oceanic crust at deformation front (Ma)	Average sediment accumulation rate (m/Ma)
Pre-collision	734	3,400	7	485 (Miocene–Quaternary)
Pre-collision	745	50	0.15	350 (Quaternary)
Collision	751	600	0.43	1400 (Quaternary)
Post-collision	769	3,300	9	365 (Miocene–Quaternary)

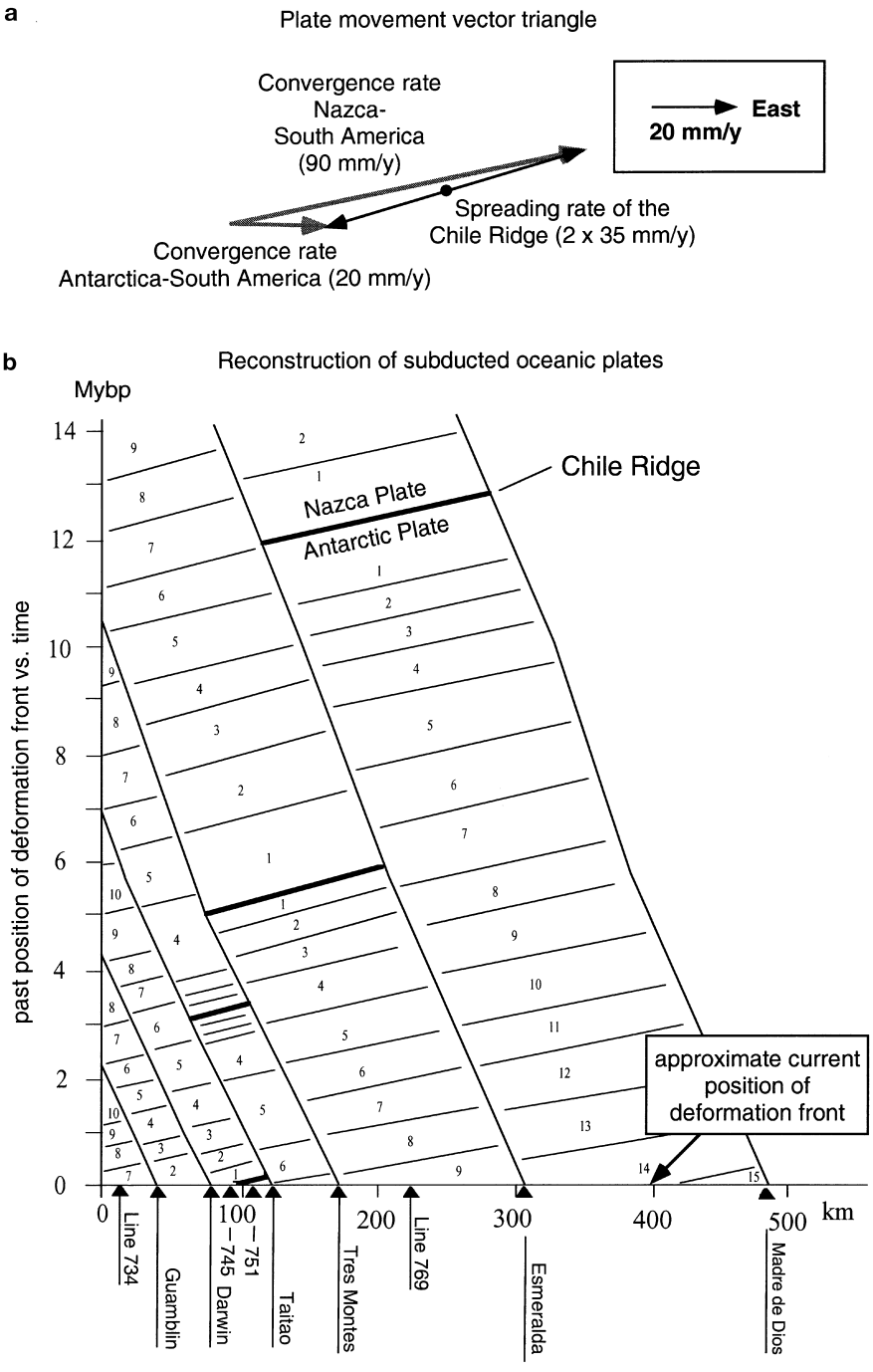

Fig. 6 **a** Vector triangle showing the plate kinematic relationship between the Chile Ridge spreading (half spreading rate 35 mm/year), and Nazca–South America (90 mm/year) and Antarctica–South America (20 mm/year) subductions; **b** Ocean floor reconstructions for the Nazca and Antarctica plates between the latitude of seismic line 734, north of the Guamblin fracture zone, and the Madre de Dios fracture zone (after Murdie et al. 1993). The horizontal axis of the diagram is oriented roughly parallel to the southern Chile trench. The vertical axis shows the retrograde age of the deformation front back to 14 Ma before present. *Numbers within the segments* are chrons, whereas the *thick line* is the spreading centre of the Chile Ridge. The age of oceanic crust presently at the deformation front as a function of latitude can be determined from the chron numbers near the horizontal axis

Table 3 Sediment accumulation rates estimated from biostratigraphic dating of ODP Leg 141 cores

Sediment accumulation rates from biostratigraphic dating of ODP Leg 141 cores along Line 745			
Time (Ma B.P.)	Site 859 (m/Ma)	Site 860 (m/Ma)	Site 861 (m/Ma)
Upper Pleistocene (0.7–present)	41	47	260
Lower Pleistocene (1.8–0.7)	–	47	44
Upper Pliocene (3.2–1.8)	287	47	203
Lower Pliocene (5.0–3.2)	–	47	–

inferred. From the plate kinematic setting it can be inferred that the Miocene sediments were deposited in a hemipelagic to pelagic setting well away from the southern Chile trench. We have no direct information from drill-holes and in the seismic sections (Fig. 2) there is no clearly identifiable 'pelagic' section at the base of the sedimentary piles. Therefore, a reliable estimate of the Miocene accumulation rates is difficult to make. Pelagic sedimentation in the world's oceanic basins away from trenches normally is at low (<50 m/Ma) rates. We therefore used the lower limit

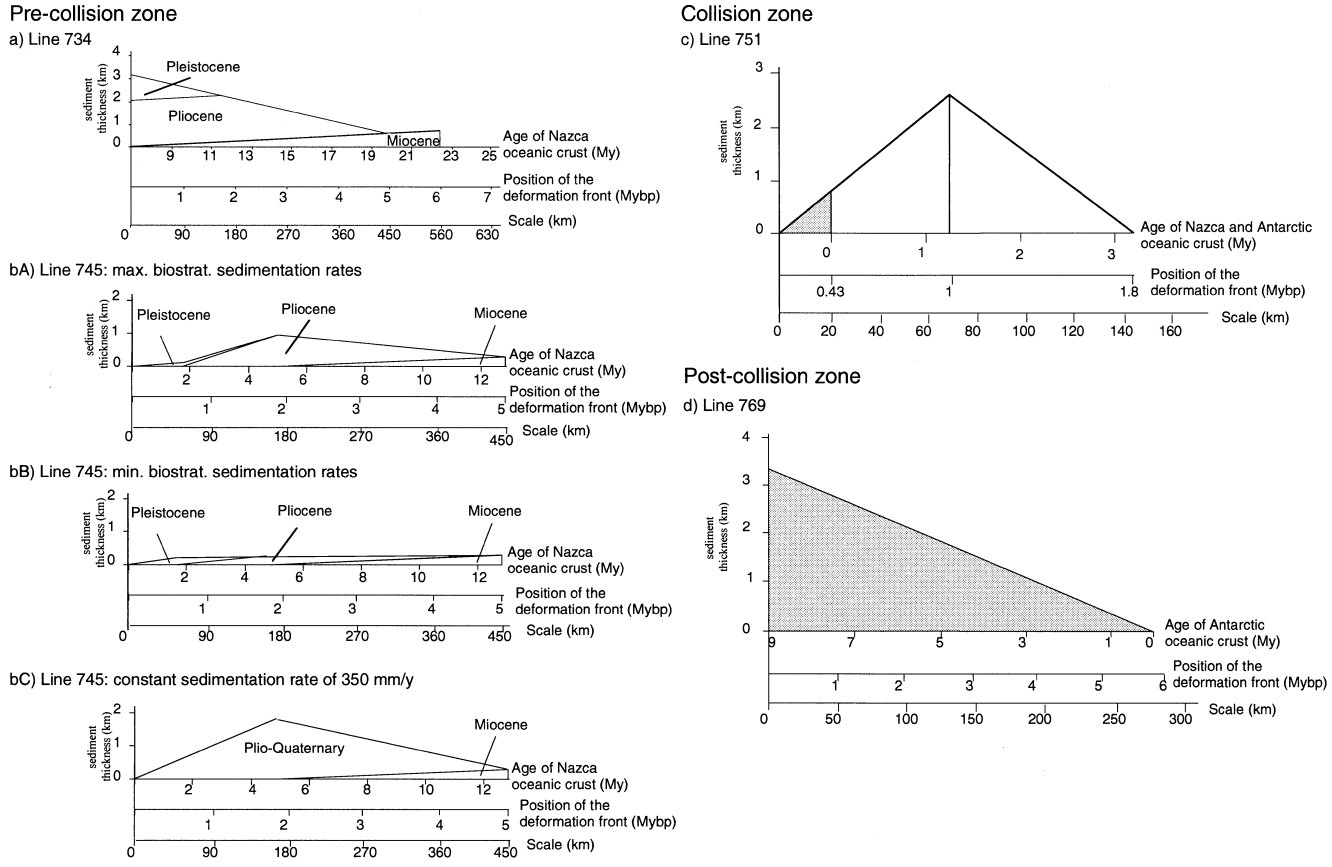

Fig. 7 Synthetic basin models, showing sediment thickness (*vertical axis*) versus age of oceanic crust, position of deformation front, and basin width (*horizontal axis*). The origin of the models is defined by the age of oceanic crust presently passing the deformation front (derived from Fig. 6b). **a** Basin model along Line 734; **bA**, **bB**, **bC** basin models along Line 745; **c** basin model along Line 751; **d** basin model along line 769 for the past 5.7 Ma. See text

of the accumulation rates based on evidence from ODP Leg 141 drill cores (i.e. 41 m/Ma) for the sedimentary input models (see below). There are several additional arguments to support this low sedimentation rate estimate: First, most of the southern Andean margin and its continental hinterland was submerged or formed part of lowlands at the time (Pankhurst et al., 1988), probably leading to low rates of terrigenous mass wasting from the continent. As shown from fission track studies on apatite (George and Hegarty 1995), the major uplift of the southern Andes (and thus a related increase in sediment input into the southern Chile trench) took place in the latest Miocene ~7 Ma before present. Second, 'empty trench scenarios' in the vicinity of modest-sized accretionary prisms are known. Off the northern Barbados Ridge accretionary complex, the sedimentary succession from Lowest Eocene to present is only 500 m thick (e.g. Mascle et al. 1988), and similar observations regarding sediment starvation were made in the Peru trench further north (von Huene et al. 1994), and in the northern Chile trench off Antofagasta (von Huene et al. 1999). Third, the balance of subducted and accreted sediments (see below) is fairly robust against inaccuracies in the estimation of the Miocene sediment contribution as it constitutes only a small fraction of the possible basin fill (Fig. 7).

The restored cross sectional areas of the basin fill were obtained by multiplying the duration of sedimentation with the accumulation rates inferred for the respective time slices (Table 2). This procedure requires steady state sedimentation for the Plio-Quaternary, an assumption that can be justified by the uplift history of the sediment source area (see discussion above). In the cases of Lines 745 and 734, 41 m/Ma of sediment accumulation was assumed for the Miocene (Fig. 7). Cross sectional areas of the sedimentary prisms in the models were calculated, and the results are given in Table 1.

Balance of subducted and accreted sediments

Next, we shall balance the volumes of sediment in the accretionary wedges and in the respective synthetic ocean basins. In this way the amount of sediment subducted along with the downgoing oceanic slab can be estimated. All sediment volumes were reduced to zero porosity using porosity–depth data from ODP Sites

Table 4 Sediment subduction, sediment subduction rates, and percentages of accretion for the southern Chile convergent margin. For Line 745 the *asterisk* denotes the data based on biostratigraphically defined sediment accumulation rates

Sediment subduction, sediment subduction rates, and percentages of accretion				
Line	Latitude (°S)	Subducted sediment (km^3/km trench) (max./min.)	Sed. subduction rate (km^3/km trench×Ma) (max./min.)	Sediment accretion (%) (max./min.)
734	44°30′	484.7/469.8	80.8/78.3	20.7/20.6
745	45°55′	321.1/293.3	64.2/58.8	12.9/12.8
745*	45°55′	76.6/7.0	15.3/1.4	81.2/38.4
751	46°15′	117.1/107.8	65.1/59.9	11.8/11.4
769	47°35′	137.8/132.4	23.0/22.1	62.8/59.7

859, 860, 861 and 863 (raw data in Behrmann et al. 1992). Exponential porosity–depth functions (Fig. 4b; e.g. Athy 1930) were fitted to the ODP Leg 141 core data. The functions vary considerably from site to site, apparently depending on deposition and diagenesis on either young, 'hot' oceanic crust in a high heat-flow regime (Sites 859, 863), or on older crust (Sites 860, 861) with lower heat flow (cf. Behrmann et al. 1992).

As very young (Line 745) or effectively zero-age (Line 751) 'hot' oceanic crust is being subducted at or near the Chile Triple Junction (see Table 2), removal of the pore space was done using the depth/porosity functions of Sites 859 and 863, respectively. In the pre-collision (Line 734) and post-collision (Line 769) zones the depth/porosity functions of sites 860 and 861 were used. In the pre-collision and post-collision zones the trench is floored by older oceanic crust (7–9 Ma; Table 2), making a more normal diagenetic and consolidation history likely. Having two functions available for each scenario we obtain 'natural' brackets for a minimum and maximum estimate of solid rock volume (Table 1). The differences between 'solid area max.' and 'solid area min.' in Table 1 are ~10%. This variation is within the range published of porosity–depth curves for hemipelagic clastics (e.g. Bray and Karig 1985; Brückmann 1989).

Now the solid-rock cross sectional areas of the accretionary wedges and the synthetic basin fills are compared for each of the four profiles studied. From Table 1 it is evident that none of the accretionary wedge sections has a 'solid rock' area as large as that of the associated basin section. In the case of Lines 734 (pre-collision zone) and 751 (collision zone) this disparity is quite large, indicating that only a small percentage (see Table 4) of the sediments carried to the convergent plate boundary by the downgoing oceanic plate have avoided subduction. Accretion percentage for Line 734 is just below 21% and for Line 751 it is only about 11–12% (Table 4). Rates of sediment subduction (Table 4) are ~80 km^3/km trench×Ma for the pre-collision zone at Line 734, and 60–65 km^3/km trench×Ma for the collision zone at Line 751. In the zone of imminent ridge collision at Line 745 estimates for the accretion behaviour of the system during the last 5 million years vary greatly. Depending on assumption of sediment accumulation rates and minimum/maximum scenarios, percentages of accretion range between ~13 and 81% (Table 4). Above, we have pointed out that the accumulation rate of 350 m/Ma from the reflection seismic data suffers from an extremely short history and is thus more uncertain than other estimates. For this reason, we prefer the 745* scenario, based on drill-hole data (Table 3), indicating accretion rates between 38 and 81%, and sediment subduction rates between 1–15 km^3/km trench×Ma. This scenario is based on accumulation rate information from drill-holes that span the whole of the 5-Ma considered in the model. At the latitude of Line 769, where ridge collision occurred 6 million years ago, and plate convergence is slower (20 mm/year), a history of rebuilding of the accretionary prism in front of the continental forearc leads to about 60–63% of sediment accretion (Table 4), and sediment subduction rates in the order of 22–23 km^3/km trench×Ma.

Discussion

From the diagrams displaying the sedimentation rates and sediment subduction rates in the vicinity of the Chile Triple Junction as a function of latitude (Fig. 8) it is evident that spreading ridge subduction induces a long-term (10-Ma time scale) change in the accretion behaviour of the southern Chile convergent margin. This is best visualized by the dramatic difference in sediment subduction rates against a background of comparable long-term sedimentation rates (compare Fig. 9a, b) for the latitudes of Lines 734 (pre-collision) and 769 (post-collision). Values of ~80 km^3 solid rock volume, which were subducted during 1 million years per kilometre of trench width at the latitude of Line 734 (as an average for the Plio-Quaternary) lie close to the maximum range of a global volume balance study by von Huene and Scholl (1991) who also took the Miocene into account. The copious influx of sediments at the latitudes of Lines 734 and 769 most probably relates to the accelerated uplift and erosion of the southern Andes since ~7 Ma B.P. and is not a direct consequence of spreading ridge subduction. Conversely, young southern Andean uplift may reflect the long-term or cyclic subduction of large volumes of trench sediments and forearc basement as part of a self-regulating process (e.g. Lallemand 1992) or, in

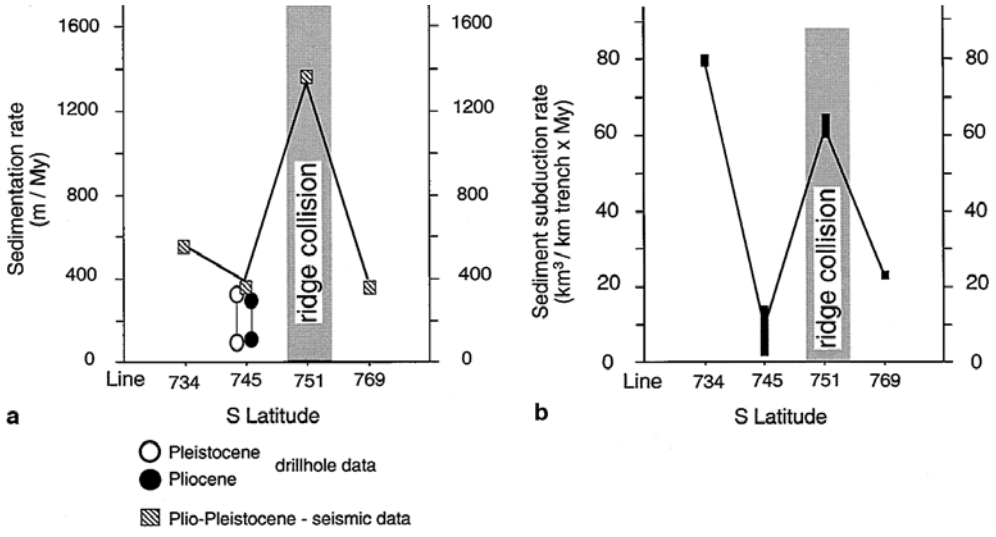

Fig. 8 Rates of **a** sedimentation, and **b** sediment subduction at the latitudes of Lines 734, 745, 751, and 769

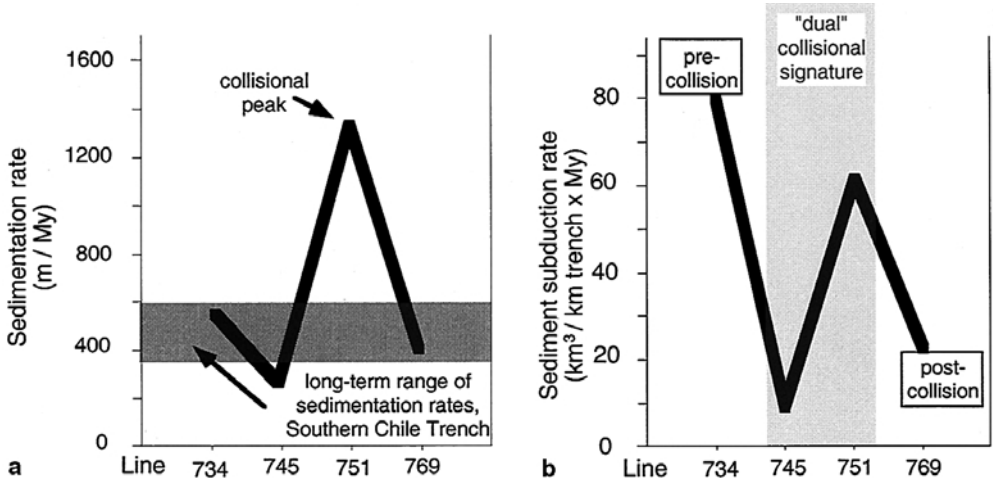

Fig. 9a, b The 'geological fingerprint' of spreading ridge subduction in terms of sedimentation rates and sediment subduction rates, as derived from this study. See text for discussion

even more general terms, to cyclicity in the behaviour of thrust wedges at convergent margins (e.g. Gutscher et al. 1996). Therefore, the view that accretion generally takes place where both a thick trench-sediment sequence is accumulated, or large accretionary prisms already exist (e.g. von Huene 1986; Davis and Hyndman 1989; Brown et al. 1990), has to be treated with caution. We shall return to this point at the end of this discussion paragraph.

If we look at the results of our study in their 'small-scale' context (i.e. within 50 km north and south of the Chile Triple Junction), some unusual coincidence is observed between the sedimentation and the subduction rates (Fig. 9a, b). Both curves reach maximum values in the collision zone at the latitude of Line 751. Increased turbidite activity triggered by tectonic movements in the oversteepened forearc is probably the cause for the very high sedimentation rate of 1,400 m/Ma (Table 2; see also Behrmann et al. 1994) observed here, although it cannot be considered a long-term characteristic. In contrast, the north-eastern flank of the Chile Ridge, which consists of 'hot', buoyant oceanic crust, reaches the trench at the latitude of Line 745 and causes forearc uplift when being subducted. In the wake of spreading ridge subduction the trench floor is no longer a distinct negative topographic feature, and hence no large volumes of sediment can be ponded there. This is reflected by the record of low sedimentation rates inferred for the Plio-Quaternary from ODP Leg 141 drill cores (41–287 m/Ma, Table 3; cf. Behrmann et al. 1992). In summary, the pair of distinct low and high sedimentation rates, and the corresponding minimum and maximum in sediment subduction rates (compare Fig. 9a, b) probably represent the geological fingerprint of spreading ridge subduction proper. This is a signal in the order of 1–5 million years duration. Large discontinuities are introduced regarding the mass flux in the subduction system: a deficit in subducted sedimentary material on the order of 100 km^3/km trench over, say, 3 million years is followed by an equally large oversupply over 1–2 million years. As much of the forearc uplift associated with spreading ridge subduction may be thermally induced, the sedimentation pattern here

is probably different to settings where aseismic ridges are subducted (e.g. the Nazca Ridge; von Huene et al. 1996).

Although sedimentation rates on the subducting plates in the collision zone are only constrained over a short time span, and cannot be more than rough approximations, it is evident that such a variation in the supply of subducted sediments and their associated fluids may be one of the factors influencing melt processes in the downgoing slab and overlying asthenospheric mantle wedge. In the search for manifestations of this process in fossil subduction settings, we must face the fact that because of the extremely short time scale for the process, it may be impossible to detect these phenomena simply because of lack of chronostratigraphic resolution.

Along Line 751 in the collision zone there is strong evidence that major volumes of basement rocks are removed from the forearc along with accreted sediments (see Figs. 2 and 3; cf. Behrmann et al. 1994). It is not easy to make an estimate, but in comparing forearc basement geometries in Fig. 5b, c, it appears that ~20–30 km^3 of basement rock may have been removed by normal faulting, forearc truncation and subduction. This is in contrast to estimates by Bourgois et al. (1996) from the Peninsula Taitao (see Fig. 1 for location), where subduction of the Chile Ridge occurred ~3 million years ago. According to Bourgois et al. (1996) subduction erosion there removed forearc basement and sediments at rates between 230 and 440 km^3/km trench×Ma. The volumetric estimates are not corrected for porosity, and rely on the assumption of a downgoing slab angle of 30° (Murdie et al. 1993) and 23 km of trench retreat, calculated from the source depth of 30 km for the magmas that created a young granodiorite pluton (Bourgois et al. 1996). The disparity between the figures in our study and those from Bourgois et al. (1996) can be explained in several ways. First, the estimated values for subduction erosion at the Peninsula Taitao rest upon precise assessment of magma source depth. An error of only few kilometres introduces large differences in the amount of trench retreat acceptable to the model. Second, the 30° dip angle for the subduction zone may be too large. Where ridges are subducted the dip commonly shallows (see data of von Huene et al. 2000; Ranero et al. 2000), and to use a general dip from earthquake locations (cf. Murdie et al. 1993) may be presumptive. Towards the hinterland the subduction zone possibly steepens, but important to calculations of erosion is the shallowly dipping frontal part. Third, at the Chile Triple Junction the process of forearc destruction is by no means completed, and large volumes of basement rocks at the latitude of Line 751 may face the fate of being subducted in the next 1 million years or so. We conclude, however, by emphasizing that sediment subduction at or near sites of active spreading ridge subduction has a dual signature: a pronounced low followed by a short-term high. From the comparison of our results with those of Bourgois et al. (1996) we conclude that subduction erosion of forearc basement may be highly variable in space and time, and can not yet be adequately understood on the basis of the data available.

A qualitative description of the tectonic consequences of spreading ridge subduction is given in the series of cartoons shown in Fig. 10. Approximately 5 million years before ridge collision (Fig. 10a), the incoming sediment on the rapidly subducting oceanic Nazca Plate is only partially accreted frontally or underplated at the base of the forearc. The 'subduction gate', or 'subduction channel' (Cloos and Shreve 1996; Gutscher et al. 1998) is open to sediments. Shortly before ridge collision (Fig. 10b), sediment subduction is greatly reduced, mainly as a consequence of lower sediment supply to the trench. In the phase of forearc destruction provoked by the collision event (Fig. 10c), basement slivers and large amounts of sediment are transported into the subduction zone on a natural conveyor belt with chain-saw topography. In $\geq$5 million years following ridge collision the destroyed and tectonically oversteepened forearc is gradually rebuilt (Fig. 10d) by the oceanward addition of a new, large accretionary wedge and forearc basin fill. In our view, the rebuilding process can be easiest understood considering thrust wedge mechanics (e.g. Davis et al. 1983; Platt 1988). Spreading ridge collision in a trench–trench-ridge triple point setting (McKenzie and Morgan 1969) necessarily goes along with a strong reduction in subduction rate (Fig. 10), and therefore lower frictional forces transmitted across the plate boundary. This allows for a lower angle of taper of the overriding forearc wedge. The lower angle of taper is then attained by successive frontal accretion of large sediment masses to the forearc.

Conclusion

Spreading ridge subduction at the southern Chile convergent margins has profound short-term (1–5 Ma) and longer-term (10 Ma) effects on the balance of sedimentation, sediment accretion and sediment subduction.

Viewed on a large and long-term scale, sediment supply to the Antarctic and Nazca oceanic basins and trenches seaward of the southern Chile forearc has been of the order of 350–500 m/Ma for the past 6–7 Ma. Prior to spreading ridge subduction about 80% of the sediment on the downgoing Nazca Plate was subducted, and only 20% was frontally accreted to the forearc north of the Chile Triple Junction. After spreading ridge subduction the destroyed southern Chile forearc south of the triple junction was rebuilt by frontal accretion of large volumes of sediment. Over 60% of the sediment on the downgoing Antarctic plate was bulldozed off by the overriding South American Plate.

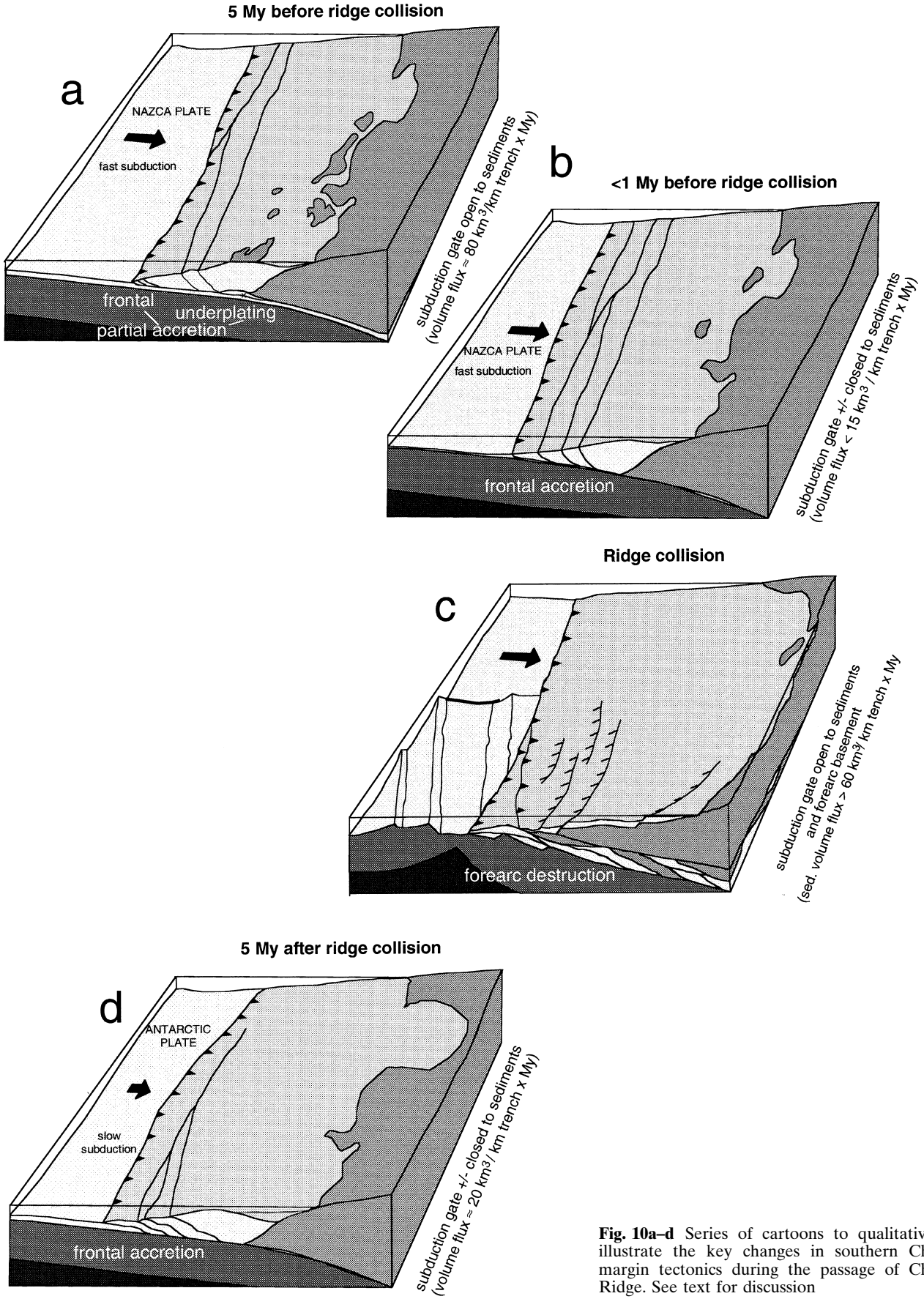

Fig. 10a–d Series of cartoons to qualitatively illustrate the key changes in southern Chile margin tectonics during the passage of Chile Ridge. See text for discussion

The shorter-term and smaller-scale expressions are a decrease in trench sedimentation rate prior to the arrival of the spreading ridge at the deformation front, and a synchronous decrease in the rate of sediment subduction. This probably relates to the disappearance of the trench as a negative topographic feature and depo-centre for large amounts of sediment. In the collision zone proper, a short-lived high peak in sedimentation rates appears because of local forearc uplift, oversteepening and erosive dissection. Sediment accretion rates are very low, and most of the incoming sediment is subducted along with major volumes of the continental forearc basement.

The dual coupling of sedimentation rates and sediment subduction rates in the course of collision may well be a 'geological fingerprint' of spreading ridge subduction. Although large volumes of rock are involved, the phenomenon may, however, be difficult to detect in fossil convergent orogens because of the limits in chronostratigraphic resolution.

Acknowledgements We thank Steve Lewis and Steven Cande for making seismic reflection data available. Reviews and critical remarks by Nathan Bangs, Peter Haeussler, Steve Lewis, Onno Oncken, Dave Scholl, Eli Silver and Roland von Huene helped to improve this manuscript and sharpened our thinking. This study was funded through Deutsche Forschungsgemeinschaft grant Be 1041/7 to J.H.B.

References

Athy LF (1930) Density, porosity, and compaction of sedimentary rocks. Bull Am Assoc Petrol Geol 14:24

Bangs NLB, Cande SC (1991) Complex structures imaged at Chile margin. JOI/USSAC Newslett 4(1):1–2

Bangs NLB, Cande SC (1997) The episodic development of a convergent margin inferred from structures and processes along the southern Chile margin. Tectonics 16:489–503

Bangs NLB, Cande SC, Lewis SD, Miller J (1992) Structural framework of the Chile Margin at the Chile Ridge collision zone. In: Behrmann JH, Lewis SD, Musgrave RJ et al. (eds) Proceedings of the Ocean Drilling Program, Initial Reports, vol 141. College Station, TX, pp 11–21

Barker PF (1982) The Cenozoic subduction history of the Pacific margin of the Antarctic Peninsula: ridge crest-trench interactions. J Geol Soc Lond 139:787–802

Beck ME Jr (1983) On the mechanism of tectonic transport in zones of oblique subduction. Tectonophysics 93:1–11

Behrmann JH, Lewis SD, Musgrave RJ, Bangs N, Bodén P, Brown K, Collombat H, Didenko AN, Didyk BM, Froelich PN, Golovchenko X, Forsythe R, Kurnosov V, Lindsley-Griffin N, Marsaglia K, Osozawa S, Prior D, Sawyer D, Scholl D, Spiegler D, Strand K, Takahashi K, Torres M, Vega-Faundez M, Vergara H, Waseda A (1992) Proceedings of the Ocean Drilling Project, Initial Reports, vol 141. College Station, TX

Behrmann JH, Lewis SD, Cande SC, ODP Leg 141 Scientific Party (1994) Tectonics and geology of spreading ridge subduction at the Chile Triple Junction: a synthesis of results from Leg 141 of the Ocean Drilling Program. Geol Rundsch 83(4):832–852

Bourgois J, Martin H, Lagabrielle Y, Le Moigne J, Frutos Jara J (1996) subduction erosion related to spreading-ridge subduction: Taitao peninsula (Chile margin triple junction area). Geology 24:723–726

Bourgois J, Guivel C, Lagabrielle Y, Calmus T, Boulègue J, Daux V (2000) Glacial–interglacial trench supply variation, spreading-ridge subduction, and feedback controls on the Andean margin development at the Chile triple junction area (45–48°S). J Geophys Res 105:8355–8386

Bray CJ, Karig DE (1985) Porosity of sediments in accretionary prisms and some implications for dewatering processes. J Geophys Res 90:768–778

Brown KM, Mascle A, Behrmann JH (1990) Mechanisms of accretion and subsequent thickening in the Barbados Ridge accretionary complex: balanced sections across the wedge toe. In: Moore JC, Mascle A, Taylor E, Underwood MB (eds) Proceedings of the Ocean Drilling Program, Scientific Results, vol 110. College Station, TX, pp 209–227

Brückmann W (1989) Typische Kompaktion mariner Sedimente und ihre Modifikation in einem rezenten Akkretionskeil (Barbados Ridge). Tübinger Geowissenschaftliche Abhandlungen A5

Cande SC (1983) Nazca–South America plate interactions 80 m.y. B.P. to present. EOS Trans Am Geophys Union 64:865

Cande SC, Leslie RB (1986) Late Cenozoic tectonics of the southern Chile Trench. J Geophys Res 91:471–496

Cande SC, Herron EM, Hall BR (1982) The early Cenozoic tectonic history of the southeast Pacific. Earth Planet Sci Lett 57:63–74

Cande SC, Leslie RB, Parra JC, Hobart M (1987) Interaction between the Chile Ridge and the Chile Trench: geophysical and geothermal evidence. J Geophys Res 92:495–520

Casey JF, Dewey JF (1984) Initiation of subduction zones along transform and accreting plate boundaries, triple junction evolution, and forearc spreading centres: implications for ophiolitic geology and obduction. In: Gass IG, Lippard SJ, Shelton AW (eds) Ophiolites and the oceanic lithosphere. Geol Soc Lond, Spec Publ 19:269–290

Chase CG (1978) Plate kinematics: the Americas, East Africa, and the rest of the world. Earth Planet Sci Lett 37:355–368

Cloos M, Shreve RL (1996) Shear-zone thickness and seismicity of Chilean- and Mariana-type subduction zones. Geology 24:107–110

Coats RR (1962) Magma type and crustal structure of the Aleutian Arc. In: McDonald GA, Kuno H (eds) Crust of the Pacific Basin. Am Geophys Union Geophys Monogr Ser 6:92–109

Davis D, Suppe J, Dahlen FA (1983) Mechanics of fold- and-thrust belts and accretionary wedges. J Geophys Res 88:1153–1172

Davis EE, Hyndman RD (1989) Accretion and recent deformation of sediment along the northern Cascadia subduction zone. Geol Soc Am Bull 101:1465–1480

DeLong SE, Fox PJ (1977) Geological consequences of ridge subduction. In: Talwani M, Pitman III WC (eds) Island arcs, deep sea trenches and back-arc basins. Maurice Ewing Series, Am Geophys Union, Washington, DC, pp 221–228

DeLong SE, Schwarz WM, Anderson RN (1979) Thermal effects of ridge subduction. Earth Planet Sci Lett 44:239–246

Flint SS, Prior DJ, Agar SM, Turner P (1994) Stratigraphic and structural evolution of the Tertiary Cosmelli Basin and its relationship to the Chile triple junction. J Geol Soc Lond 151:251–268

Flueh ER, Shipboard Scientific Party SO 103 (1995) Cruise Report SO 103, CONDOR 1B, Valparaiso-Valparaiso. GEOMAR Report 41

Flueh ER, Vidal N, Ranero CR, Hojka A, von Huene R, Bialas J, Hinz K, Cordoba D, Danobeitia JJ, Zelt C (1998) Seismic investigation of the continental margin off- and onshore Valparaiso, Chile. Tectonophysics 288:251–263.

Forsythe RD, Prior D (1992) Cenozoic continental geology of South America and its relations to the evolution of the Chile triple junction. In: Behrmann JH, Lewis SD, Musgrave RJ et al. (eds) Proceedings of the Ocean Drilling Project, Initial Reports, vol 141, College Station, TX, pp 23–31

Forsythe RD, Nelson EP, Carr MJ, Kaeding ME, Hervé M, Mpodozis CM, Soffia JM, Harambadour S (1986) Pliocene near trench magmatism in southern Chile: a possible manifestation of ridge collision. Geology 14:23–27

George AD, Hegarty KA (1995) Fission track analysis of detrital apatites from Sites 859, 860 and 862, Leg 141 Ocean Drilling Program. In: Lewis SD, Behrmann JH, Musgrave RJ, Cande SC et al. (eds) Proceedings of the Ocean Drilling Project, Scientific Results, vol 141, College Station, TX, pp 181–192

Gutscher M-A, Kukowski N, Malavieille J, Lallemand SE (1996) Cyclical behaviour of thrust wedges: insights from high basal friction sandbox experiments. Geology 24(2):135–138

Gutscher M-A, Malavieille J, Lallemand S, Collot J-Y (1999) Tectonic segmentation of the North Andean Margin: impact of the Carnegie Ridge collision. Earth Planet Sci Lett 168:255–270

Haeussler PJ, Bradley DC, Goldfarb RJ, Snee LW, Taylor C (1995) Link between ridge subduction and gold mineralization in southern Alaska. Geology 23:995–998

Herron EM, Cande SC, Hall BR (1981) An active spreading center collides with a subduction zone: a geophysical survey of the Chile Margin triple junction. Geol Soc Am Mem 154:683–701

Hilde TWC (1983) Sediment subduction versus accretion around the Pacific. Tectonophysics 99:381–397

Howell DG (1989) Tectonics of suspect terranes, mountain building and continental growth. Chapman and Hall, London

Huene R von (1986) To accrete or not accrete, that is the question. Geol Rundsch 75:1–15

Huene R von, Lallemand S (1990) Tectonic erosion along the Japan and Peru convergent margins. Geol Soc Am Bull 102:704–720

Huene R von, Scholl DW (1991) Observations at convergent margins concerning sediment subduction, subduction erosion, and the growth of continental crust. Rev Geophys 29:279–316

Huene R von, Kukowski N, Pecher IA (1994) Tectonics, subduction erosion, and accretionary history of the Peruvian continental margin. Terra Nostra 2/94:40

Huene R von, Pecher IA, Gutscher M-A (1996) Development of the accretionary prism along Peru and material flux after subduction of Nazca Ridge. Tectonics 15:19–33

Huene R von, Corvalan J, Flueh ER, Korstgard J, Ranero CR, Weinrebe W, Condor Scientists (1997) CONDOR, a study of the Nazca Plate and adjacent Andean margin off Valparaiso, Chile. Tectonics 16(3):474–488

Huene R von, Weinrebe W, Heeren F (1999) Subduction erosion along the North Chile margin. J Geodyn 27:345–358

Huene R von, Ranero CR, Weinrebe W (2000) Quaternary convergent margin tectonics of Costa Rica, segmentation of the Cocos Plate, and Central American volcanism. Tectonics 19:314–334

Hussong DM, Edwards PB, Johnson SH, Campbell JF, Sutton GH (1976) Crustal structure of the Peru–Chile trench: 8°–12°S latitude. In: Sutton GH, Manghani MH, Moberly R (eds) The geophysics of the Pacific Ocean basin and its margin, vol 19. Geophys Monogr Ser. Am Geophys Union, Washington, DC, pp 71–85

Karig DE, Sharman III GF (1975) Subduction and accretion in trenches. Earth Planet Sci Lett 86:377–389

Klitgord KD, Mudie JD, Larson PA, Grow JA (1973) Fast sea floor spreading on the Chile Ridge. Earth Planet Sci Lett 20:90–93

Kopf A (1995) Feststoffbilanzierung akkretierten und subduzierten Sediments und computergestützte Rückwärtsmodellierung deformierter Krustenquerschnitte am Kontinentalrand von Südchile. Quantitative geometrische und kinematische Rekonstruktion der Forearc-Entwicklung nahe dem Chile-Tripelpunkt (Ocean Drilling Program Leg 141). Giessener Geol Schriften, no 55

Kukowski N, von Huene R, Malavieille J, Lallemand SE (1994) Sediment accretion against a buttress beneath the Peruvian continental margin at 12°S as simulated with sandbox modeling. Geol Rundsch 83(4):822–831

Lagabrielle Y, Le Moigne J, Maury RC, Cotten J, Bourgois J (1994) Volcanic record of the subduction of an active spreading ridge, Taitao peninsula (southern Chile). Geology 22:515–518

Lallemand SE (1992) Transfer de matière en zone de subduction. Habilitation à diriger des recherches. Mèm Sci Terre Univ PM Curie Paris, reg no 92-27

Marshak S, Karig DE (1977) Triple junctions as causes of anomalous near trench igneous activity between the trench and the volcanic arc. Geology 5:233–236

Mascle A, Moore JC Taylor E, Andreieff P, Alvarez F, Barnes R, Beck C, Behrmann J, Blanc G, Brown K, Clark M, Dolan J, Gieskes J, Fisher A, Hounslow M, McLellan P, Moran K, Ogawa Y, Sakai T, Schoonmaker J, Vrolijk P, Wilkens R, Williams C (1988) Proceedings of the Ocean Drilling Program, Initial Reports, vol 110, College Station, TX

McKenzie DP, Morgan WJ (1969) Evolution of triple junctions. Nature 224:125–133

Miller H (1970) Das Problem des hypothetischen 'Pazifischen Kontinentes' gesehen von der chilenischen Pazifikküste. Geol Rundsch 59:927–938

Minster JB, Jordan TH (1978) Present-day plate motions. J Geophys Res 83:5331–5354

Murauchi J (1971) The renewal of island arcs and the tectonics of marginal seas. In: Asano S, Udintsev GB (eds) Island arc and marginal sea. Proceedings of the 1st Japan–USSR Symposium on Solid Earth Sciences. Tokai Univ Press, Tokyo, pp 39-56

Murdie RE, Prior DJ, Styles P, Flint SS, Pearce RG, Agar SM (1993) Seismic responses to ridge-transform subduction: Chile triple junction. Geology 21:1095–1098

Pankhurst RJ, Hole MJ, Brook M (1988) Isotope evidence for the origin Andean granites. Trans R Soc Edinb Earth Sci 79:123–133

Pankhurst RJ, Hervé F, Rojas L, Cembrano J (1992) Magmatism and tectonics in continental Chiloé, Chile (42°–42.3°S). Tectonophysics 205:283–294

Platt JP (1988) The mechanics of frontal imbrication: a first-order analysis. Geol Rundsch 77:577–589

Platt JP, Leggett JK, Young J, Raza H, Alam S (1985) Large-scale sediment underplating in the Makran Accretionary Prism, southwest Pakistan. Geology 13:507–511

Ramos VA, Kay SM (1992) Southern Patagonian plateau basalts and deformation: backarc testimony of ridge collisions. Tectonophysics 205:261–282

Ranero CR, von Huene R, Flueh E, Duarte M, Baca D, McIntosh K (2000) A cross section of the convergent Pacific margin of Nicaragua. Tectonics 19:335–357

Rutland RWR (1971) Andean orogeny and ocean floor spreading. Nature 233:252–255

Scholl DW, Marlow MS, Cooper AK (1977) Sediment subduction and offscraping at Pacific margins. In: Talwani M, Pitman WC III (eds) Island arcs, deep sea trenches and back-arc basins. Maurice Ewing Series 1, Am Geophys Union, Washington, DC, pp 199–210

Scholl DW, von Huene R, Vallier TL, Howell DG (1980) Sedimentary masses and concepts about tectonic processes at underthrust ocean margins. Geology 8:564–568

Sisson VB, Hollister LS, Onstott TC (1989) Petrologic and age constraints on the origin of a low-pressure/high-temperature metamorphic complex, southern Alaska. J Geophys Res 94:4392–4410

Willett SD (1992) Dynamic and kinematic growth and change of a Coulomb Wedge. In: McClay KR (ed) Thrust tectonics. Chapman and Hall, London, pp 19–32